PHYSICAL REVIEW B **82**, 125327 (2010)

Valence-band splitting energies in wurtzite InP nanowires: Photoluminescence spectroscopy and *ab initio* calculations

E. G. Gadret,[1] G. O. Dias,[1] L. C. O. Dacal,[2,3] M. M. de Lima, Jr.,[2] C. V. R. S. Ruffo,[1] F. Iikawa,[1] M. J. S. P. Brasil,[1] T. Chiaramonte,[1] M. A. Cotta,[1] L. H. G. Tizei,[1] D. Ugarte,[1] and A. Cantarero[2]
[1]*Instituto de Física "Gleb Wataghin," UNICAMP, Campinas, SP, Brazil*
[2]*Instituto de Ciencia de los Materiales, Universidad de Valencia, Valencia, Spain*
[3]*Instituto de Estudos Avançados (IEAv)-CTA, São José dos Campos, SP, Brazil*
(Received 1 July 2010; revised manuscript received 2 September 2010; published 29 September 2010)

We investigated experimentally and theoretically the valence-band structure of wurtzite InP nanowires. The wurtzite phase, which usually is not stable for III-V phosphide compounds, has been observed in InP nanowires. We present results on the electronic properties of these nanowires using the photoluminescence excitation technique. Spectra from an ensemble of nanowires show three clear absorption edges separated by 44 meV and 143 meV, respectively. The band edges are attributed to excitonic absorptions involving three distinct valence-bands labeled: A, B, and C. Theoretical results based on "*ab initio*" calculation gives corresponding valence-band energy separations of 50 meV and 200 meV, respectively, which are in good agreement with the experimental results.

DOI: 10.1103/PhysRevB.82.125327 PACS number(s): 78.67.Uh, 71.20.Nr, 61.46.Km

I. INTRODUCTION

Nanoscale semiconductor materials offer many possibilities to investigate fundamental physics based on quantum phenomena and also to develop novel technological applications. In particular, semiconductor nanowires (NWs) have attracted great attention in recent years. Investigation of NWs revealed remarkable structural results, such as the occurrence of the wurtzite (WZ) crystal structure on arsenide and phosphide III-V compounds.[1–5] Typically, this phase is not present in their bulk counterparts, which crystallize in the zinc-blende (ZB) structure.[6] Glas *et al.*[5] have demonstrated that the vapor-liquid-solid (VLS) growth mode favors the WZ phase along the [0001] direction as compared to [111] ZB phase because the surface energy of certain crystal plans are lower under this phase as compared to the ZB structure. Furthermore, the occurrence of stacking faults is very frequent during the growth of NWs, resulting in alternations between the ABAB… stacking sequence (for the WZ phase along the [0001] axis) to the ABCABC… sequence (for the ZB phase along the [111] axis).[1,7,8] This type of polytypism has been previously reported for InP NWs (Refs. 7–9) and should give rise to a quantum confinement effect along the wire due to the larger energy band gap of WZ InP as compared to the ZB InP [(~80 meV) (Refs. 3 and 10)]. Moreover, the interface band lineup of this structure is predicted to be type II,[11] as illustrated in the diagram of Fig. 1. Recent works discuss the effects of polytypism on the optical properties in InP NWs.[7–9] Nonetheless, few reports have focused on the details of the electronic structure of WZ InP. In contrast to the ZB phase, the valence band of WZ semiconductors splits in 3 bands, the so called A, B, and C bands [see Fig. 2(b)]. The energies of those bands are still unknown for InP.

Due to the low carrier recombination velocity of surface states,[12–14] InP NWs present a relatively strong optical emission. Therefore, optical techniques are very practical to characterize those structures. In this work, we present results concerning the valence band structure of WZ InP NWs, including experimental results using optical spectroscopy and theoretical calculations based on "*ab initio*" methods. We obtained a very good agreement between experiment and theory.

II. EXPERIMENTAL DETAILS

The NWs were grown on (001) GaAs substrates by the VLS method in a chemical beam epitaxy (CBE) system. We used gold nanoparticles (diameter of ~25 nm) as the catalyst. NWs were grown at 420 °C and three different trimethyl-indium (TMIn) fluxes, 0.15 (sample S1), 0.3 (S2), and 0.45 sccm (S3), respectively.

The optical measurements include microphotoluminescence (micro-PL) to analyze single NWs and excitation photoluminescence (PLE) from ensemble of NWs. The micro-PL setup was homemade using an optical microscope

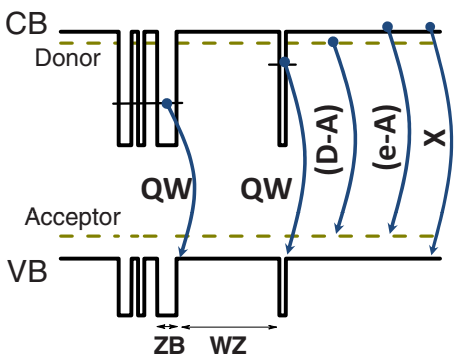

FIG. 1. (Color online) Schematic (not in scale) of the potential profile of InP polytypelike structure in ZB and WZ phases. The arrows represent the optical transitions: QW for the multiquantum well transitions, (e-A) and (D-A) for the band-acceptor and donor-acceptor recombination, respectively, and X for the exciton recombination in WZ InP.

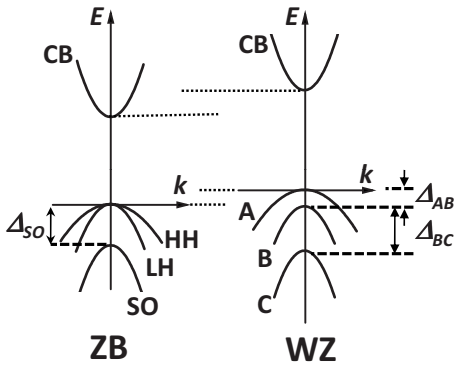

FIG. 2. Schematic (not in scale) of the band structure of InP in ZB and WZ phases.

objective (50×) and a solid state laser (532 nm) for excitation. The detection was performed using a 0.5 m single monochromator with a charge-coupled device detector (Andor). The samples were cooled using a cold-finger He cryostat. For PLE, we used a tungsten lamp coupled to a 0.5 m single monochromator, as the excitation light, and a 0.75 m double monochromator with a S1 photomultiplier, for detection. The samples were cooled using a He gas cryostat at 6 K. A homemade photoacoustic photodetector with a mineral coal sensor was used to calibrate the intensity of the incident excitation intensity at each wavelength. For micro-PL measurements, NWs were mechanically transferred to an Al-coated GaAs substrate. The Al film was used to avoid a background signal from the substrate and also to increase the visual contrast between NWs and substrate.

III. THEORY

Figure 2 depicts schematic band-structure diagrams for ZB and WZ InP considering a wave vector $k \sim 0$. The low-temperature band gap of ZB InP is well known, $E_g = 1.423$ eV.[6] For the WZ phase, the reported value is slightly larger, ~80 meV, as observed by PL measurements.[3,10] The spin-orbit valence-band splitting energy for ZB InP is $\Delta_{SO} = 110$ meV.[6] For the WZ phase, there are two splitting energies for the valence band, Δ_{AB} and Δ_{BC}, corresponding to the energy separation at $k=0$ between bands A and B, and B and C, respectively.

In order to estimate the valence band splitting energies we have performed *ab initio* calculations of the InP band structure in WZ phase. We employed the "*full potential linearized augmented plane wave method*" as implemented in the WIEN2K code[15] with the Perdew-Burke-Ernzerhof functional for exchange and correlation in the "*generalized gradient approximations*." Our optimized structure presented a WZ phase lattice parameter $a_{WZ}=a_{ZB}/\sqrt{2}$, where $a_{ZB}=5.8697$ Å is the lattice constant of ZB InP.[6,16] For the "*c*" parameter we obtained 6.912 Å, a deviation of 2% from the ideal c/a ratio. The calculated splitting energies are presented in Table I where the fundamental energy gap is omitted due to the well known underestimation given by *ab initio* calculations.[17]

The Bloch component of the wave function of the hole in the valence band is strongly polarized in the WZ structure.

TABLE I. Absorption edge values (corresponding to the peak energies of the PLE spectra), E_A, E_B, and E_C, obtained at 6 K and experimental and theoretical values of valence band splitting energies for WZ InP.

	E_A (eV)	E_B (eV)	E_C (eV)	Δ_{AB} (meV)	Δ_{BC} (meV)
Exper. PLE	1.488	1.532	1.675	44	143
Theory				50	200

Our calculations show that bands A and B are polarized along the (0001) plane while band C is polarized perpendicular to this plane. Due to the symmetry of the conduction-band wave function, the optical emission and absorption involving those bands should, therefore, be linearly polarized following the polarization of the valence-band wave function. Transitions involving bands A and B are thus allowed for light polarized along the (0001) plane, while for band C, the light should be polarized along the *c* axis. For micro-PL measurements performed at normal incidence, the NWs were positioned laying at the Al-coated substrate surface. For this configuration, transitions involving all three valence bands are allowed using the appropriate configuration for the linear polarization.

IV. EXPERIMENTAL RESULTS AND DISCUSSIONS

Transmission electron microscopy (TEM) images show that the WZ is the dominant phase for our NWs and the wire axis is oriented along the [0001] axis. Furthermore, we observed stripes of ZB InP (oriented along the [111]) along the wire length, as described above. The thickness of the ZB phase stripes varies from one to several monolayers and they are randomly distributed along the wire. The density of the stacking faults increases with an increasing TMIn flux. In particular, for the smaller TMIn flux (sample S1), stacking faults are statistically insignificant. While for the sample with intermediate TMIn flux (sample S2), we observed a few number of stacking faults for each of the analyzed wires by TEM. In general, the NWs present a needlelike shape, where the largest diameter ranges from 50–100 nm and the thinner one, approaches the gold nanoparticle diameter (~25 nm). The NWs are usually 5–10 μm long.

Figure 3 shows a series of micro-PL spectra from NWs grown at different conditions and measured using two excitation powers and two linear polarizations, parallel and perpendicular to the growth axis of the NWs. We have measured several NWs (approximately 5) for each sample, whereas we only present a limited number of representative spectra in Fig. 3. Under a low-excitation power regime (100 nW, left column in Fig. 3), except of NW1 of S3, all other NWs of Fig. 3 are dominated by a main emission band centered at ~1.44 eV with a weaker shoulder at the low-energy side. This emission appears at intermediate energies between the ZB [1.421 eV (Ref. 6)] and the WZ [~1.489 eV (Refs. 3 and 10)] InP band-gap energies. Similar results were reported by several works (Refs. 7 and 8), and the band was attributed to a recombination involving confined levels on the multi-

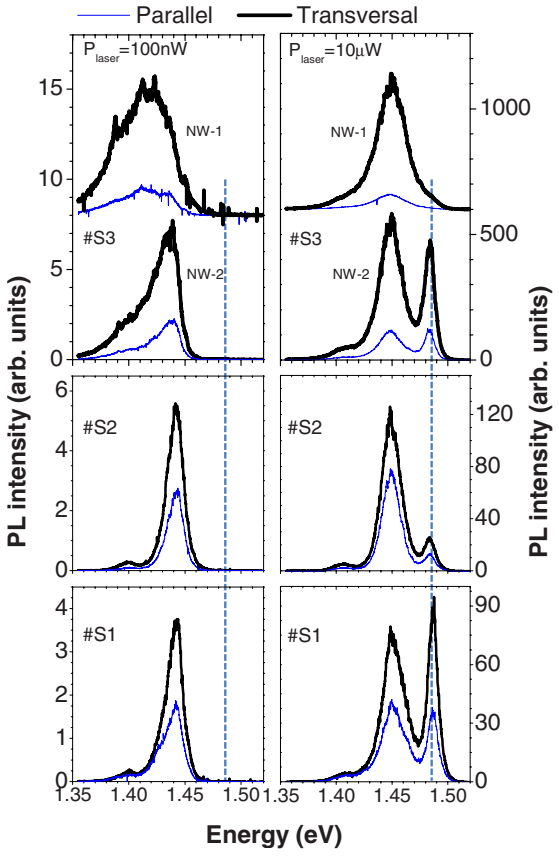

FIG. 3. (Color online) Micro-PL spectra of several single NWs measured for 100 nW (left column) and 10 μW (right column) laser powers and two components of linear polarization of light, parallel and transversal to the NWs. The vertical dashed lines indicate the exciton recombination energy in WZ InP. For sample S3 we present the spectra for two distinct NWs, where the NW-1 PL spectra were vertically shifted by adding a constant.

QWs formed by the ZB-WZ polytypism (Fig. 1). However, this interpretation is not consistent with the observation of this band on samples with low densities of stacking faults, specially sample S1 which wires are essentially in the WZ phase. The fact that this emission band is observed at nearly the same energy and with similar linewidths for a large number of wires, including samples with rather distinct characteristics, suggests that this recombination involves bulk-related states, such as impurities. Based on this hypothesis, we should observe a saturation of this band with increasing excitation intensities. Indeed, for high excitation powers (10 μW, right column of the Fig. 3), we observe the emergence of an additional emission band at higher energies, at $\sim$1.488 eV, slightly smaller than the expected band gap of WZ InP. An emission with similar energy was previously observed on InP NWs and it was attributed to excitons on bulklike WZ InP.[3,10] The energy separation between those two emission bands ($\sim$50 meV) is compatible with the binding energy of an acceptor impurity in InP. Therefore, we attribute the 1.44 eV emission to a band-acceptor (e-A) and donor-acceptor (D-A) recombination in WZ InP. This type of recombination is usually followed by optical phonon replicas. In fact, we observe a weak emission $\sim$40 meV below the 1.44 band, which is in good agreement with the longitudinal optical phonon mode observed in the Raman spectra of our NWs (not shown here). The most likely shallow acceptor in our NWs is carbon,[18] as this element is abundant in the CBE system with chemical sources.

We remark that the PL spectra from sample S3 are slightly different from the other two samples. The main emission band becomes broader so that the low-energy shoulder attributed to a phonon replica is no longer well resolved. This result indicates an additional emission in the energy range of 1.40–1.44 eV. The intensity of this additional emission varies for different wires measured from this sample, in such a way that the PL spectrum can be very similar from the S1 and S2 PL spectra or become a rather broad band, as the case of the NW1. Considering that sample S3 has a larger density of stacking faults, the additional emission can thus be related to multi-QW (MQW) recombination emission, as suggested by previous works.[7,8]

Figure 3 shows that all emission bands from the NWs are strongly polarized along the direction perpendicular to the wire. The resulting linear polarization degree ($\rho_{linear}=\frac{I_T-I_P}{I_T+I_P}$, where I_T and I_P are the PL intensity for light polarized transversal and parallel to the wire, respectively) varies from wire to wire but we did not observe a clear correlation with the TMIn flux. The observed linear polarization of the emission along the (0001) plane is consistent with the Bloch function polarization predicted for the WZ A-valence-band. Similar results have also been reported by Mishra *et al.*[10]

We point out that most of the NWs investigated by micro-PL (laser spot of $\sim$2 μm) have relatively large diameters, typically $\sim$100 nm, which is much larger than the Bohr´s radius in InP ($\sim$9 nm). Therefore, lateral confinement is negligible for those NWs. On the other hand, polytypism can introduce multiquantum wells that should confine the carriers along the wire axis, as discussed above. Pemasiri *et al.*[8] observed rather long decay times and large blueshifts with increasing excitation intensities of the PL emission from their NWs, which were interpreted as evidence of the type-II character of the PL emission. In our case, the 1.44 eV emission band also shows a blueshift with increasing excitation powers, but its shift ($\sim$3 meV per decade of excitation power) is, however, much smaller than previously reported values (over 10 meV/decade[7,8]). Furthermore, a blueshift is also expected for a donor-acceptor recombination. The results thus corroborate our attribution of the main emission band from our NWs to an impurity-related recombination on WZ InP.

Figure 4 shows the PL and a series of PLE spectra for NWs ensembles. The measurements were performed on as-grown samples, where the NWs are randomly oriented relative to the GaAs substrate. The PLE spectra shown in Fig. 4 were obtained by measuring the emission intensity at the peak of the main PL emission band. We assume here that the hole relaxation from A, B, and C valence bands to the acceptor impurity level is faster than its recombination, as it is expected for bulk materials. Measurements at different detection energies were also performed and will be discussed later. Due to the high density of NWs, the emission from the GaAs substrate is relatively weak as compared to the NWs. None-

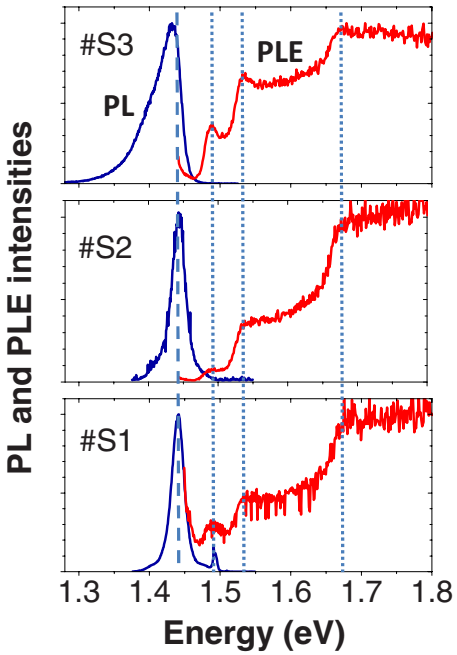

FIG. 4. (Color online) Normalized PL (blue lines) and PLE (red lines) spectra of three samples grown at different TMIn flux. The vertical dashed line was plotted to guide the eyes only. The dotted lines indicate the absorption edges. PL spectra were measured using the 532 nm line from a solid state laser.

theless, depending on the density and distribution of NWs along the sample we might observe some emission from the GaAs substrate, such as the sharp emission line at ~1.49 eV observed in the PL spectrum of sample S1 and attributed to a GaAs donor-acceptor recombination. It is interesting to notice that the PL spectra from the ensembles of NWs presented in Fig. 4 are actually very similar to those shown in Fig. 3 for single NWs, including their line widths. The result demonstrates that the broadening of the optical emission is established by a single wire, in the case of samples S1 and S2, due to impurity-related broadening, and in the case of S3, due to the fluctuations of the MQW structure within a single NW.

We also observed from Fig. 4 that the energy separation between the lowest absorption edge from the PLE spectra and the PL peak (Stokes shift) is relatively large, ~50 meV, which indicates a different nature for the emission and the absorption processes. In fact, the first absorption edge occurs at the same energy of the high-energy emission band observed by micro-PL measurements under high-excitation regime (Fig. 3), that was attributed to the excitonic recombination on bulklike WZ InP. This result is consistent with WZ being the dominant phase of our NWs and, therefore, having the largest density of states. All PLE spectra present three absorption edges at constant energies for all samples, which indicate that absorption occurs through common levels to all samples. Furthermore, the constant energies indicate the absence of confinement effects on the absorption levels. The

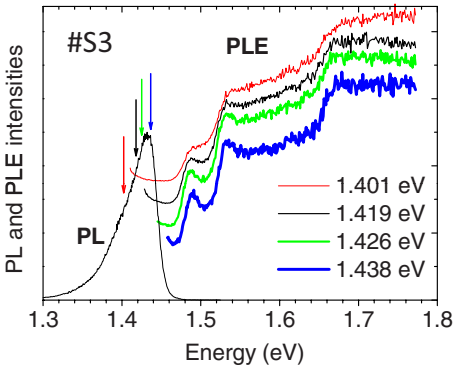

FIG. 5. (Color online) Detection dependence of normalized PLE spectra. All spectra were shifted along the vertical axis. The detection positions are indicated by arrows at the PL spectrum.

three observed edges are then attributed to transitions between the three split valence bands and the conduction band of bulk WZ InP. The experimental energies of the three absorption edges and their energy separation are presented in Table I. The obtained splitting energies are in very good agreement with the calculated ones, which corroborates our assignment. Notice that some absorption edges in Fig. 4 present excitoniclike features (peaks), especially in the case of the sample S3 grown with the highest TMIn flux. The fact that the excitonic character is stronger for some samples is still not clear.

We also investigated the PLE measurements as a function of the detection energy. The results for sample S3 are shown in Fig. 5. Excitoniclike PLE peaks are quite evident for detection at high energies while PLE spectra show steplike edges when the signal is detected at lower energies. Nonetheless, the edge energies remain basically unaltered as the detected energy is changed, which reinforces the conclusion that the joint density of states is dominated by bulk WZ InP. Therefore, the excitonic character of the absorption level varies from sample to sample and also as a function of the emission energy, which the origin is still under investigation.

V. CONCLUSIONS

We presented experimental and theoretical results for the valence-band splitting energies of InP in the wurtzite phase. These parameters have never been reported before. They are, however, fundamental for the optical properties of InP NWs and, therefore, of large interest for the development of device applications based on those structures.

ACKNOWLEDGMENTS

Financial support from CNPq, FAPESP, and bilateral CAPES (Brazil)/MICINN (Spain), Contract No. MAT2009–10350, is acknowledged. We also acknowledge LNLS, Brazil, for granting access to the electron microscopy facilities. We thank H. Obata for assistance in sample growth and M. M. Tanabe for technical support.

[1] M. Koguchi, H. Kakibayashi, M. Yazawa, K. Hiruma, and T. Katsuyama, Jpn. J. Appl. Phys. **31**, 2061 (1992).
[2] B. Mandl, J. Stangl, T. Martensson, A. Mikkelsen, J. Eriksson, L. S. Karlsson, G. Bauer, L. Samuelson, and W. Seifert, Nano Lett. **6**, 1817 (2006).
[3] M. Mattila, T. Hakkarainen, M. Mulot, and H. Lipsanen, Nanotechnology **17**, 1580 (2006).
[4] T. Akiyama, K. Nakamura, and T. Ito, Phys. Rev. B **73**, 235308 (2006).
[5] F. Glas, J.-C. Harmand, and G. Patriarche, Phys. Rev. Lett. **99**, 146101 (2007).
[6] *Numerical Data and Functional Relationships in Science and Technology*, Landoldt Börnstein, New Series, Group III Vol. 17a, edited by O. Madelung (Springer-Verlag, Berlin, 1982), p. 281.
[7] J. Bao, D. C. Bell, F. Capasso, J. B. Wagner, T. Mårtensson, J. Trägårdh, and L. Samuelson, Nano Lett. **8**, 836 (2008).
[8] K. Pemasiri, M. Montazeri, R. Gass, L. M. Smith, H. E. Jackson, J. Yarrison-Rice, S. Paiman, Q. Gao, H. H. Tan, C. Jagadish, X. Zhang, and J. Zou, Nano Lett. **9**, 648 (2009).
[9] D. Spirkoska, J. Arbiol, A. Gustafsson, S. Conesa-Boj, F. Glas, I. Zardo, M. Heigoldt, M. H. Gass, A. L. Bleloch, S. Estrade, M. Kaniber, J. Rossler, F. Peiro, J. R. Morante, G. Abstreiter, L. Samuelson, and A. Fontcuberta i Morral, Phys. Rev. B **80**, 245325 (2009).
[10] A. Mishra, L. V. Titova, T. B. Hoang, H. E. Jackson, L. M. Smith, J. M. Yarrison-Rice, Y. Kim, H. J. Joyce, Q. Gao, H. H. Tan, and C. Jagadish, Appl. Phys. Lett. **91**, 263104 (2007).
[11] M. Murayama and T. Nakayama, Phys. Rev. B **49**, 4710 (1994).
[12] K. T. Tsen, G. Halama, O. F. Sankey, S.-C. Y. Tsen, and H. Morkoç, Phys. Rev. B **40**, 8103 (1989).
[13] K. Tai, R. Hayes, S. L. McCall, and W. T. Tsang, Appl. Phys. Lett. **53**, 302 (1988).
[14] E. Yablonovitch, R. Bhat, C. E. Zah, T. J. Gmitter, and M. A. Koza, Appl. Phys. Lett. **60**, 371 (1992).
[15] P. Blaha, K. Schwarz, G. K. H. Madsen, D. Kvasnicka, and J. Luitz, *WIEN2k, An Augmented Plane Wave Plus Local Orbitals Program for Calculating Crystal Properties*, edited by Karlheinz Schwarz (Technical Universität Wien, Austria, 2001).
[16] I. Vurgaftman, J. R. Meyer, and L. R. Ram-Mohan, J. Appl. Phys. **89**, 5815 (2001).
[17] F. Tran and P. Blaha, Phys. Rev. Lett. **102**, 226401 (2009).
[18] B. J. Skromme, G. E. Stillman, J. D. Oberstar, and S. S. Chan, J. Electron. Mater. **13**, 463 (1984).